Title	Preparation of tetrabutylammonium salt of a mono-Ru(III)-substituted α-Keggin-type silicotungstate with a 4,4′-bipyridine ligand and its electrochemical behaviour in organic solvents
Auther(s)	Ogo, Shuhei; Moroi, Sachie; Ueda, Tadaharu; Komaguchi, Kenji; Hayakawa, Shinjirou; Ide, Yusuke; Sano, Tsuneji; Sadakane, Masahiro
Citation	Dalton Transactions , 42 (19) : 7190 - 7195
Issue Date	2013
DOI	10.1039/c3dt50300c
Self DOI	
URL	http://ir.lib.hiroshima-u.ac.jp/00045957
Right	Copyright (c) Royal Society of Chemistry 2013 This is not the published version. Please cite only the published version. この論文は出版社版でありません。引用の際には出版社版をご確認ご利用ください。
Relation	

Journal Name

Dynamic Article Links ►

Cite this: DOI: 10.1039/c0xx00000x

www.rsc.org/xxxxxx

ARTICLE TYPE

Preparation and structural characterisation of tetrabutylammonium salt of mono-ruthenium(III)-substituted α-Keggin-type silicotungstates with 4,4'-bipyridine ligand and its electrochemical behaviour in organic solvents.

Shuhei Ogo,[1] Sachie Moroi,[1] Tadaharu Ueda,[2] Kenji Komaguchi,[1] Shinjiro Hayakawa,[1] Yusuke Ide,[1] Tsuneji Sano[1] and Masahiro Sadakane*[1,3]

Received (in XXX, XXX) Xth XXXXXXXXX 20XX, Accepted Xth XXXXXXXXX 20XX

DOI: 10.1039/b000000x

Tetrabutylammonium (TBA) salt of mono-ruthenium(III)-substituted α-Keggin-type silicotungstates with a 4,4'-bipyridine (bipy) ligand, $TBA_5[\alpha\text{-}SiW_{11}O_{39}Ru^{III}(bipy)]$ (**1**), which is soluble in various organic solvents, was prepared by cation exchange reaction of $Cs_5[\alpha\text{-}SiW_{11}O_{39}Ru^{III}(bipy)]$ with tetrabutylammonium bromide. The compound **1** was characterised using IR, ^{1}H-NMR, elemental analysis, single crystal X-ray analysis, X-ray absorption near-edge structure (XANES) analysis (Ru L_3-edge), electron spin resonance (ESR), cyclic voltammetry (CV) and UV-Vis. Single crystal X-ray analysis of **1** revealed that the Ru^{III} unit was incorporated in the α-Keggin-type silicotungstate framework and coordinated by a bipy molecule through a Ru-N bond. CV indicated that the incorporated Ru^{III}-bipy was reversibly oxidised to the Ru^{IV}-bipy derivative and reduced to the Ru^{II}-bipy derivative in organic solvents. The redox potential of $Ru^{IV/III}$-bipy was found to be affected by organic solvents. Moreover, Ru^{V}-bipy derivative was observed in acetonitrile.

Introduction

Polyoxometalates (POMs) are discrete metal-oxide clusters of W, Mo, V and Nb that have been attracting increasing interest because of their multi-electronic redox activities and their photochemical, acidic, and magnetic properties, resulting in potential applications of POMs as catalysts and functional materials.[1-7] Keggin-type heteropolytungstates are polyoxotungstates containing one central heteroatom X surrounded by 12 condensed W-O octahedra to form $[XW_{12}O_{40}]^{n-}$ (X= P (n = 3), Si (n = 4), Ge (n = 4), etc.). It is possible to substitute one W with Ru to form mono-Ru-substituted Keggin-type heteropolytungstates such as $[XW_{11}O_{39}Ru(L)]^{n-}$ (X= P, Si or Ge). The heteropolytungstates act as pentadentate ligands to Ru. The heteropolytungstate ligands stabilise a higher valence of Ru compared to organo-ruthenium complexes with pyridine-based ligands,[8, 9] which are often used as redox catalysts.[6, 7] Catalytic activities of mono-Ru-substituted heteropolytungstates for the oxidation of cyclooctene,[10] water[11-13] and alcohols[14, 15] and for the reduction of dimethylsulfoxide[8] and carbon dioxide[16] have been reported.

It is well known that the redox potential of POMs depends on negative charges of POMs, kind of counter cations and pH of solution.[17-23] It is also known that the redox potentials of POMs are affected by anion solvation.[18, 19, 24-26] Keita and Nadjo's group reported that the first one-electron reduction potentials of $[SiW_{12}O_{40}]^{4-/5-}$ and $[P_2W_{18}O_{62}]^{6-/7-}$ were shifted to more positive potentials with increases in Gutmann acceptor number[27] of the solvent.[24] Bond's group reported that reversible redox potentials for $[S_2W_{18}O_{62}]^{4-/5-}$ and $[S_2Mo_{18}O_{62}]^{4-/5-}$ in water and ionic liquids were significantly more positive than those in acetonitrile and dichroromethane.[25, 26, 28, 29] Steckhan's group reported that the addition of organic solvents to water shifted the redox potential towards more negative values.[30] More positive redox potentials were observed in higher Lewis acidic solvents (i.e., larger acceptor number). These phenomena were attributed to solvent stabilisation of the more highly charged reduced forms of POMs, which were stronger Lewis bases than the corresponding oxidised form.[17, 19, 24-26, 31]

The importance of the donor property of solvents for redox potentials of POMs was also reported. Small cations, such as H^+, Li^+ and Na^+, were more strongly associated with the reduced forms of POMs than with the corresponding oxidised form and caused changes in redox potentials and/or number of transferred electrons.[20-23, 31, 32] Himeno's group reported that the solvation ability to small cations increased with increase in the Lewis basicity (≈ donor number) of solvents and that the solvation of cations caused weakening of the interaction between the small cations and POMs.[21, 22]

Thus, the redox potential changes for POM anions are rationalized in terms of the electron donor-acceptor concept of the solvent.[20-22] In the course of our research using Ru-substituted polyoxometalates, we have been interested in the solvent effect on redox behaviour of the incorporated Ru. Redox potentials of

Ru-substituted heteropolytungstates in an organic solvent have been reported, but the solvent effect has not yet been reported.[14, 33] From the point of view of practical applications of POMs in catalytic organic synthesis and materials science, it should be of considerable significance to extensively study the electrochemical properties of POMs in organic solvents.

Here we report the preparation and characterisation of tetrabutylammonium (TBA) salt of Ru^{III}-substituted α-Keggin-type silicotungstates with a 4,4'-bipyridine (bipy) ligand, $TBA_5[\alpha\text{-}SiW_{11}O_{39}Ru^{III}(bipy)]$ (**1**). This compound was soluble and stable in various organic solvents, which enabled us to study the electrochemical behaviour of **1** in organic solvents.

Experimental Section

Materials

All chemicals were reagent-grade and used as supplied. Homemade de-ionized water (Millipore, Elix) was used. The compound $Cs_5[\alpha\text{-}SiW_{11}O_{39}Ru^{III}(bipy)]\cdot 8H_2O$ (bipy: 4,4'-bipyridine) was prepared according to the published procedure[9] and analysed by CV, IR and UV-Vis.

Preparation of tetrabutylammonium (TBA) salt of $[\alpha\text{-}SiW_{11}O_{39}Ru^{III}(bipy)]^{5-}$ (1)

$Cs_5[\alpha\text{-}SiW_{11}O_{39}Ru^{III}(bipy)]\cdot 8H_2O$ (0.230 g, 0.0609 mmol) dissolved in water (22 mL) was added to an aqueous solution (20 mL) containing tetrabutylammonium bromide (0.0982 g, 0.305 mmol). After the resulting brownish solution had been heated at 80 ºC for 3 hours, the reaction mixture was cooled down to room temperature and filtered. The filtrate was extracted with 7 mL of chloroform three times. After the chloroform solution had been evaporated by a rotary evaporator, a red paste was obtained (yield: 0.195 g, 77%). This red paste was dissolved in acetonitrile (20 mL), and then a vessel containing the acetonitrile solution was placed in a closed beaker containing diethylether at room temperature. After several days, red solid **1** was obtained, and it was filtered and air-dried (yield: 0.123 g, 49%). Same recrystallisation was repeated to obtain plate-like red crystals which were suitable for single crystal structural analysis.

Elemental analysis (C, H, N) for $(Bu_4N)_5[SiW_{11}O_{39}Ru(C_{10}H_8N_2)]\cdot CH_3CN$, found: C, 26.3; H, 4.7; N, 2.6 %; calcd: C, 26.4; H, 4.6; N, 2.7 %. IR spectrum (ν_{max}/cm^{-1}): 1637 (m), 1595 (m), 1528 (w), 1484 (m), 1408 (w), 1380 (m), 1153 (w), 1107 (w), 1065 (w), 1025 (m), 954 (s), 909 (vs), 872 (s), 786 (vs). Cyclic voltammograms (acetonitrile): $E_{1/2}$ ($Ru^{V/IV}$) = 884 mV, $E_{1/2}$ ($Ru^{IV/III}$) = -122 mV and $E_{1/2}$ ($Ru^{III/II}$) = -1220 mV vs. Fc^+/Fc. ^{1}H-NMR (CD_3CN): (δ/ppm) 6.927 (br, 2H), 6.274 (br, 2H), 3.325 (br, 40H), 1.776 (br, 40H), 1.511 (br, 40H), 1.053 (br, 60H) (cf. 1.976 for C*H*D_2CN).

X-ray crystallography

Single-crystal X-ray diffraction data of a crystal (0.30×0.20×0.05 mm) were collected with a Rigaku R-AXIS RAPID II diffractometer at 93 K using multi-layer mirror monochromated Mo-K_α radiation (λ = 0.71075 Å). All calculations were performed using the CrystalStructure[34] crystallographic software package except for refinement, which was performed using SHELX-97.[35] All non-hydrogen atoms (W, Ru, Si, O, N, C) were refined anisotropically. The hydrogen atoms of the bipyridine ligand and acetonitrile molecules were placed geometrically using a riding model. The H atoms of TBA cations could not be located. The high residual electron density in the structure (the highest peak 9.62 e·Å^{-3}) was located exclusively near the tungsten atoms. Crystallographic data are summarized in Table 1. The number of acetonitrile molecules determined by XRD was slightly larger than that determined by elemental analysis, probably due to the loss of acetonitrile in the drying process before elemental analysis.

Crystallographic data for the structure reported in this paper has been deposited with the Cambridge Crystallographic Data Centre (CCDC) as supplementary publication no. CCDC-922096. Copy of the data can be obtained free of charge on application to CCDC, 12 Union Road, Cambridge CB2 1EZ, UK [fax.: (internat.) +44 1223/336-033; email: deposit@ccdc.cam.ac.uk].

Table 1 Crystal data and structure refinement of $(Bu_4N)_5[SiW_{11}O_{39}Ru(bipy)]\cdot 3.5CH_3CN$ (**1**)

Empirical formula	$C_{194}H_{58}N_{21}O_{78}Ru_2Si_2W_{22}$
Molecular weight / g·mol^{-1}	8191.37
Crystal colour and shape	Red, plate
Temperature / K	93(1)
Crystal system	Triclinic
Space group (no.)	*P*-1 (2)
a / Å	20.3725(4)
b / Å	27.4946(5)
c / Å	28.3758(6)
α / °	89.680(6)
β / °	70.539(5)
γ / °	70.719(5)
Volume /Å^3	14047.9(9)
Z	2
Data / parameters	64219 / 2769
R(int)	0
Density (calcd) / g·cm^{-3}	1.936
Abs coefficient / mm^{-1}	9.155
R_1 ($I > 2\sigma(I)$) [a]	0.0791
wR_2 (all data) [b]	0.2445

[a] $R_1 = \Sigma||F_o| - |F_c|| / \Sigma|F_o|$. [b] $R_w = [\Sigma w(F_o^2 - F_c^2)^2] / \Sigma[w(F_o^2)^2]^{1/2}$.

Electrochemical measurements

Cyclic voltammetric measurements in various organic solvents were carried out at 25 ± 1 ºC with a Bioanalytical Systems (BAS) 50 W electrochemical workstation. A standard three-electrode arrangement was employed with a BAS glassy carbon disk electrode (GCE) having a surface area of 0.071 cm^2 as the working electrode, a platinum wire as the counter electrode and a silver wire electrode as a pseudo-reference electrode. Unless otherwise noted, the voltage scan rate was set at 100 mV s^{-1}. The potentials in all voltammetric experiments were converted using data derived from the oxidation of Fc (Fc/Fc^+ (Fc = ferrocene)) as an external reference. Before all measurements, the GCE was polished with 0.1 μm diamond slurry and washed with the solvents, and the sample solution was always purged with nitrogen gas for at least 5 min in order to remove the dissolved oxygen. Approximate formal potential values $E_{1/2}$ were calculated from the cyclic voltammograms as the average of cathodic and anodic peak potentials for corresponding oxidation and reduction waves.

Other analytical techniques

IR spectra were recorded on a Thermo Fisher Scientific

NICOLET 6700 FT-IR spectrometer as KBr pellets. UV-Vis spectra were recorded at ambient temperature using a Shimadzu UV-2550 double-beam spectrophotometer with a 1 mm quartz cell. Elemental analyses (C, H, N) were performed by the Natural Science Center for Basic Research and Development (N-BARD), Hiroshima University. ^{1}H-NMR spectra were recorded on a Varian system 500 (500 MHz) spectrometer (H resonance frequency: 499.827 MHz). The spectra were referenced to internal C*H*D$_2$CN (1.976 ppm).

Results and Discussion

Preparation and isolation of tetrabutylammonium (TBA) salt of [α-SiW$_{11}$O$_{39}$Ru^{III}(bipy)]$^{5-}$ (1)

Caesium salt of Cs$_5$[α-SiW$_{11}$O$_{39}$Ru^{III}(bipy)] prepared according to the published procedure[9] were exchanged with tetrabutylammonium (TBA) cations by addition of five equivalents of tetrabutylammonium bromide to an aqueous solution of the caesium salt. After recrystallisation from an acetonitrile-diethyl ether mixed solution, red crystals of TBA$_5$[α-SiW$_{11}$O$_{39}$Ru^{III}(bipy)] (**1**) were obtained.

Structural characterisation of TBA salt of [α-SiW$_{11}$O$_{39}$Ru^{III}(bipy)]$^{5-}$ (1)

Fig. S1 shows an FT-IR spectrum of **1** together with those of Cs$_5$[SiW$_{11}$O$_{39}$Ru^{III}(bipy)],[9] Cs$_5$[SiW$_{11}$O$_{39}$Ru^{III}(H$_2$O)],[13, 36] tetrabutylammonium bromide (TBABr) and 4,4'-bipyiridine. The IR spectrum of **1** was very similar to that of caesium salt of [α-SiW$_{11}$O$_{39}$Ru^{III}(bipy)]$^{5-}$ [9] with peaks corresponding to tetrabutylammonium cations at around 1500-1350 cm^{-1}, indicating that **1** contains the [α-SiW$_{11}$O$_{39}$Ru^{III}(bipy)] unit and tetrabutylammonium cations. Moreover, it was confirmed that the valence of the ruthenium ion in **1** was +3 by using the Ru-L$_3$-edge X-ray adsorption near-edge spectra (XANES) technique (Fig. S2). Elemental analysis results also indicated that the obtained compound was (Bu$_4$N)$_5$[SiW$_{11}$O$_{39}$Ru^{III}(bipy)] (**1**).

Single-crystal XRD revealed that the polyanions **1** comprised a mono-Ru-substituted α-Keggin-type silicotungstate decorated by a 4,4'-bipyridine ligand (Fig. 1a). The ruthenium (III) ion was fully incorporated into the Keggin unit via five oxygen atoms. The bond lengths between the Ru^{III} ion and the oxygen atoms of the inner SiO$_4$ group Ru–O(Si) (2.127(12) Å) were significantly shorter than the other 11 W–O(Si) bonds (2.323(11) – 2.372(9) Å). An additional site in the coordination environment of the ruthenium centre was occupied by an N atom of the bipyridine ring (Ru–N: 2.020(17) Å). These bond lengths were similar to bond lengths (Ru-O(Si): 2.120(15) Å, Ru-N: 2.05(2) Å) of the caesium salt of [α-SiW$_{11}$O$_{39}$Ru^{III}(bipy)]$^{5-}$.[9]

The bond valence sum (BVS) values[37] for the eleven W centres in **1** were in the range of 5.81 - 6.30 and the values for the Si centres were 4.11 and 4.06, suggesting formal valences of VI and IV for the W and Si atoms in **1**, respectively.

There were four independent molecules in one unit cell, and no π-π interaction between bipyridine ligands was observed in a single crystal of **1** (Fig. 1b), while bipyridine moieties in the crystal of caesium salts were linked via π-π stacking interactions of bipyridine.[9] The torsion angles of two pyridine rings in the crystal of **1** were 36.12 º (∠C(5)-C(1)-C(6)-C(10)) and 36.79 º (∠C(2)-C(1)-C(6)-C(7)), which were significantly larger than those in the crystal of caesium salt (10.79 º and 17.07 º). An asymmetric unit contained two polyanions, ten tetrabutylammonium cations (Bu_4N^+) and seven crystallization CH_3CN molecules. The TBA cations and the CH_3CN molecules fill the voids in the polyanions packing (Fig. S3).

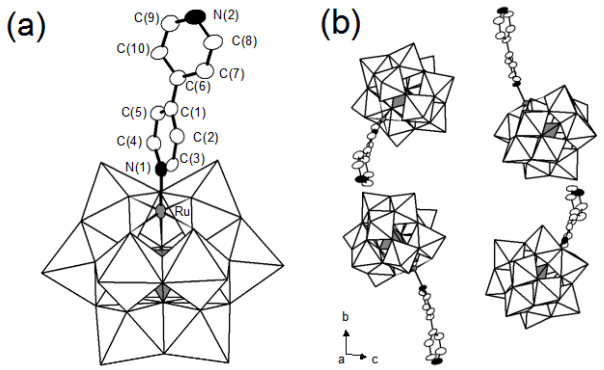

Fig. 1. (a) Combined polyhedral/thermal-ellipsoid representation of **1**. Colour code: C white, N black and Ru grey ellipsoids, SiO$_4$ grey tetrahedral and WO$_6$ white octahedral; (b) packing of compound **1** viewed along the *a* axis.

Fig. S4 shows the ^{1}H-NMR spectrum of **1** dissolved in d-acetonitrile. Six broad ^{1}H-NMR signals were observed at 6.93, 6.27, 3.33, 1.78, 1.51 and 1.05 ppm with the respective integration ratio of 1:1:20:20:20:30. The ^{1}H-NMR spectrum showed peak broadening due to the paramagnetic effect by Ru^{III}. Since a similar peak broadening was observed for TBA cation in TBA$_4$[γ-SiV$^{IV}_2$W$_{10}$O$_{36}$(μ-OH)$_4$] (3.16, 1.64, 1.40 and 0.98 ppm in CD$_3$CN),[38] the four large ^{1}H-NMR signals at 3.33, 1.78, 1.51 and 1.05 ppm were assignable to the TBA cation in **1**. It was considered that the two small signals at 6.93 and 6.27 ppm were assignable to two protons (H(7) and H(8)) in the bipyridine ligand. Although the bipyridine ligand has four asymmetric protons (H(2), H(3), H(7) and H(8)), it was considered that the signals of two asymmetric protons (H(2) and H(3)) close to paramagnetic Ru^{III} were not observed due to the strong paramagnetic effect by Ru^{III}.[9] The integration ratio of peak H(7) or H(8) to the peak at 3.33 ppm (NC*H*$_2$-) was 1:20, indicating that the molar ratio of the bipyridine ligand to TBA cation was 1:5 in the compound **1**.

Fig. S5 shows the ESR spectra of **1** in acetonitrile, acetone, *N,N*-dimethylformamide (DMF) and dimethylsulfoxide (DMSO) at 77 K. All ESR spectra showed three major lines, which were characteristic of a rhombic system as expected, and spectra were similar to those reported for TBA$_4$[PW$_{11}$O$_{39}$Ru^{III}(L)] (L = H$_2$O, pyridine and DMSO).[33, 39] Experimental ESR parameters estimated by spectral simulations (Table S1) indicated that the g_{iso} values were almost the same in these solvents. These results indicated that the ruthenium ions in **1** had a +3 oxidation state in the tested organic solvents and that the bipyridine ligand was not exchanged with organic solvents (Table S2).

Electrochemical and spectroscopic behaviour of TBA$_5$[α-SiW$_{11}$O$_{39}$Ru^{III}(bipy)] in organic solvents

Fig. 2 shows cyclic voltammograms of 0.5 mM solutions of **1** in acetonitrile, acetone, DMF and DMSO. In the case of acetonitrile solution, two well-defined redox pairs ($E_{1/2}$ = -122 and -1220 mV) were observed. The peak separations of the well-defined

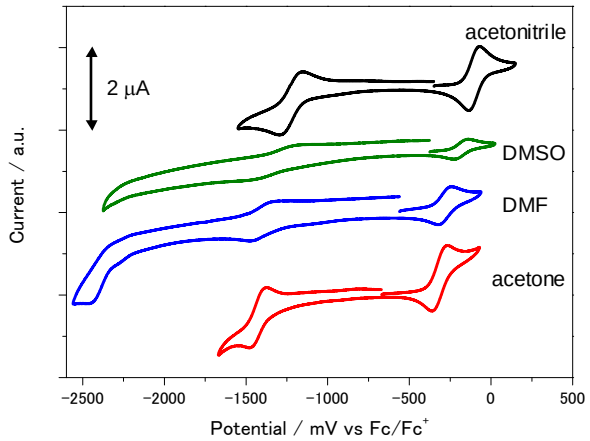

Fig. 2. Cyclic voltammograms of **1** in various organic solvents (0.1 M [*n*-Bu_4N][PF_6]). The potential first scanned positively, starting from the rest potential.

Table 2 Summary of characterisation data of **1** in various organic solvents together with solvent parameters (values from Ref. [27, 41]).

Organic solvents[a]	$E_{1/2}(Ru^{IV/III})$ / mV vs Fc/Fc^+	Diffusion coefficient / 10^{-6} cm s^{-1}	AN[b]	DN[c]	Viscosity[41]
Acetone	-306	4.05	12.5	17.0	0.303
DMF	-257	2.15	16.0	26.6	0.802
DMSO	-173	0.74	19.3	29.8	1.99
Acetonitrile	-122	8.53	19.3	14.1	0.341

[a] DMF: *N*,*N*-dimethylformamide and DMSO: dimethylsulfoxide.
[b] Acceptor number.[27] [c] Donor number.[27]

redox process at $E_{1/2}$= -122 and -1220 mV were 70 and 80 mV, respectively, and these values were almost the same as that obtained for the reversible Fc/Fc^+ one-electron-redox process under the same condition. Therefore, small departures from ideality were attributed to uncompensated resistance rather than to quasi reversibility.[28] The electrode process at $E_{1/2}$= -122 and -1220 mV should be ascribed to reversible one-electron transfer[40] for $Ru^{IV/III}$-bipy and $Ru^{III/II}$-bipy redox couples, respectively.

As shown in Fig. 2, a well-defined one-electron reversible redox pair for $Ru^{IV/III}$-bipy was observed in all tested solvents. The $E_{1/2}$ values for $Ru^{IV/III}$-bipy did not change with increase in the scan rate up to 500 mV s^{-1}. The oxidation peak currents of $Ru^{IV/III}$-bipy were linearly dependent on the square root of the scan rate (Fig. S6), thereby indicating that the electrode processes were diffusion-controlled.[40] As shown in Table 2, diffusion coefficients of **1**, calculated from the Randles-Sevcik equation, depended on the viscosity of the solvents.

The $Ru^{IV/III}$-bipy redox couple was chosen as a means of exploring the solvent effect. The redox potentials of $Ru^{IV/III}$-bipy in the organic solvents are summarized in Table 2 together with solvent parameters.[27, 41] The redox potential shifted to more positive potential in the following order: acetone (-306 mV) < DMF (-257 mV) < DMSO (-173 mV) < acetonitrile (-122 mV). It could be considered that the acceptor number of the solvents affected the redox potentials (Fig. S7).

Solvents affect the formal redox potentials of many redox-active compounds in a variety of ways, and the potential shifts can be explained in terms of solvent parameters such as acceptor or donor numbers.[27, 42] It is expected that organic solvents interacted with the anionic heteropolytungstate ligand, not with the incorporated Ru, because Ru was already coordinated by a bipyridine ligand. In the system reported here, more positive redox potentials of $Ru^{IV/III}$-bipy were observed in higher Lewis acidic solvents (larger acceptor number). This phenomenon was attributed to solvent stabilisation of the more highly charged reduced form, $[SiW_{11}O_{39}Ru^{III}(bipy)]^{5-}$, which was a stronger Lewis base than the corresponding oxidised form, $[SiW_{11}O_{39}Ru^{IV}(bipy)]^{4-}$.[18, 24]

It was reported that rexox potential of $Ru^{III/II}$ and UV-Vis absorption spectra were related.[43] In the case of Ru^{II}-polypyridyl complexes with anionic ligands (CN^- and NO_2^-), it was reported that solvents affected on not only redox potentials but also absorption spectra (d → π* MLCT bands or π → π* transitions).[43, 44] The MLCT bands of these complexes were shifted toward a shorter wavelength with increases in the solvent acceptor number.[43, 44]

Fig. 3 shows the UV-Vis spectra of **1** dissolved in the solvents. The absorption bands in the visible region may be overlapping of several absorption bands of d → π* MLCT bands, d → d transitions, etc. Because of the overlapping of two or more absorption peaks, the solvent effects on λ_{max} of the absorption bands could not be compared. However, both the absorption bands and the solution colour changed with changes in the solvents (Fig. S8). This might be due to changes in the stabilisation of d-level (Ru^{III}) by changes in interactions between **1** and solvents. The UV-Vis spectra were almost the same after storing six months (Fig. S9), indicating **1** was stable in these solvents. Further investigation is now underway in our group.

In the case of acetonitrile, a new well-defined redox pair at $E_{1/2}$ = 884 mV was observed in a more positive region (Fig. 4). The peak separation of the redox pair at $E_{1/2}$ = 884 mV was ca. 120 mV, indicating that this redox process was an electrochemically quasi-reversible redox process.[40] This redox couple could be attributed to the one-electron redox step of $Ru^{V/IV}$-bipy by comparing the peak current with the one-electron redox peak current. In the case of an aqueous solution, the $Ru^{V/IV}$ redox peak could not be detected due to overlapping with that of electrochemical water oxidation (Fig. S10).

Conclusions

The tetrabutylammonium (TBA) salt of Ru^{III}-bipy (4,4'-bipyridine)-substituted α-Keggin-type silicotungstate, $TBA_5[\alpha\text{-}SiW_{11}O_{39}Ru^{III}(bipy)]$, was prepared by cation exchange reaction using $Cs_5[\alpha\text{-}SiW_{11}O_{39}Ru^{III}(bipy)]$ and tetrabutylammonium bromide. It was confirmed by using the ESR and Ru-L_3-edge XANES tequniques that the valence of the ruthenium ion in compound **1** in solution and in the solid state should be +3. Single-crystal X-ray structural analysis revealed that polyanion $[\alpha\text{-}SiW_{11}O_{39}Ru^{III}(bipy)]^{5-}$ existed as monomers in the solid state, where no π-π interaction between individual Ru^{III}-bipy units was observed. The incorporated Ru^{III}-bipy moiety was reversibly oxidised to the Ru^{IV}-bipy derivative and reduced to the Ru^{II}-bipy derivative in the tested organic solvents. The ruthenium could be further oxidised to Ru^{V}-bipy in acetonitrile solution. The redox potential of $Ru^{IV/III}$-bipy shifted to a more positive potential with increases in the solvent acceptor number, which might be due to increasing stabilisation of the Ru^{III} species. The information

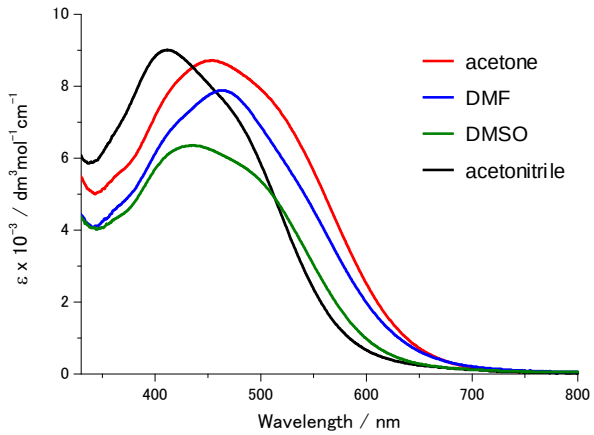

Fig. 3. UV-Vis spectra of **1** in various organic solvents.

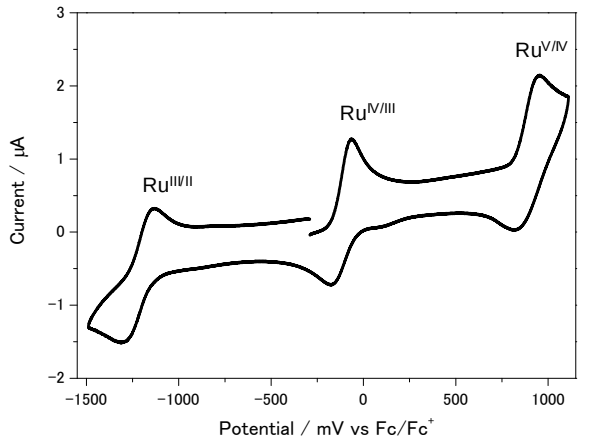

Fig. 4. Cyclic voltammogram of **1** in acetonitrile (0.1 M [*n*-Bu_4N][PF_6]). The potential first scanned positively, starting from the rest potential.

presented here is valuable for expanding the possibility of utilising these redox active POMs as redox catalysts and functional materials.

Acknowledgement

This research was supported by the JST, PRESTO program. We thank Dr. A. Yamano, X-ray Research Laboratory, Rigaku Corporation for collecting the single crystal X-ray diffraction data and help with the structural analysis. We thank Dr. Y. Mouri, the Natural Science Center for Basic Research and Development (N-BARD), Hiroshima University for the measurement of C, H and N contents. Experiments at Hiroshima Synchrotron Orbital Radiation (HiSOR) were carried out under the approval of the Hiroshima Synchrotron Radiation Center (HSRC).

Notes and references

1) Department of Applied Chemistry, Graduate School of Engineering, Hiroshima University, 1-4-1 Kagamiyama, Higashi-Hiroshima, 739-8527, Japan sadakane09@hiroshima-u.ac.jp
2) Department of Chemistry, Faculty of Science, Kochi University, 2-5-1 Akebono-cho, Kochi 780-8520, Japan
3) Japan Science and Technology Agency (JST), PRESTO, 4-1-8 Honcho, Kawaguchi, Saitama, 332-0012, Japan

† Electronic Supplementary Information (ESI) available: Experimental ESR parameters (Table S1 and S2). FT-IR spectra of **1** (Fig. S1). Normalized Ru-L_3-edge XANES spectra of **1** (Fig. S2). Packing of crystal **1** (Fig. S3). ^{1}H-NMR spectrum of **1** (Fig. S4). ESR spectra of **1** in various organic solvents (Fig. S5). Oxidation peak currents of $Ru^{IV/III}$-bipy in various organic solvents plotted against (scan rate)$^{1/2}$ (Fig. S6). Relationship between the redox potential of $Ru^{IV/III}$ and the solvent acceptor number (Fig. S7). Photograph of **1** dissolved in various organic solvents (Fig. S8). UV-Vis spectra of **1** in various organic solvents after storing six months (Fig. S9). CV and DPV curve of $Cs_5[SiW_{11}O_{39}Ru(bipy)]$ in 0.5 M KH_2PO_4 aqueous solution (Fig. S10). See DOI: 10.1039/b000000x/

1. C. L. Hill, *Special Thematic Issue on Polyoxometalates*, *Chem. Rev.*, 1998, **98**.
2. M. T. Pope, *Heteropoly and Isopoly Oxometalates*, Springer-Verlag, Berlin, 1983.
3. N. Mizuno, K. Kamata, S. Uchida and K. Yamaguchi, *Modern heterogeneous oxidation catalysis: design, reactions and characterization, ed N. Mizuno*, Wiley-VCH, Weinheim, 2009.
4. D. L. Long, R. Tsunashima and L. Cronin, *Angew. Chem. Int. Ed.*, 2010, **49**, 1736.
5. A. Proust, R. Thouvenot and P. Gouzerh, *Chem. Commun.*, 2008, 1837.
6. N. V. Izarova, M. T. Pope and U. Kortz, *Angew. Chem. Int. Ed.*, 2012, **51**, 9492.
7. P. Putaj and F. Lefebvre, *Coord. Chem. Rev.*, 2011, **255**, 1642.
8. C. Rong and M. T. Pope, *J. Am. Chem. Soc.*, 1992, **114**, 2932.
9. M. Sadakane, S. Moroi, Y. Iimuro, N. Izarova, U. Kortz, S. Hayakawa, K. Kato, S. Ogo, Y. Ide, W. Ueda and T. Sano, *Chem. Asia. J.*, 2012, **7**, 1331.
10. A. Bagno, M. Bonchio, A. Sartorel and G. Scorrano, *Eur. J. Inorg. Chem.*, 2000, 17.
11. M. Murakami, D. Hong, T. Suenobu, S. Yamaguchi, T. Ogura and S. Fukuzumi, *J. Am. Chem. Soc.*, 2011, **133**, 11605.
12. M. Sadakane, N. Rinn, S. Moroi, H. Kitatomi, T. Ozeki, M. Kurasawa, M. Itakura, S. Hayakawa, K. Kato, M. Miyamoto, S. Ogo, Y. Ide and T. Sano, *Z. Anorg. Allgem. Chem.*, 2011, **637**, 1467.
13. S. Ogo, M. Miyamoto, Y. Ide, T. Sano and M. Sadakane, *Dalton Trans.*, 2012, **41**, 9901.
14. A. Yokoyama, K. Ohkubo, T. Ishizuka, T. Kojima and S. Fukuzumi, *Dalton Trans.*, 2012, **41**, 10006.
15. K. Yamaguchi and N. Mizuno, *New J. Chem.*, 2002, **26**, 972.
16. A. M. Khenkin, I. Efremenko, L. Weiner, J. M. L. Martin and R. Neumann, *Chem. Eur. J.*, 2010, **16**, 1356.
17. I. M. Mbomekalle, X. Lopez, J. M. Poblet, F. Secheresse, B. Keita and L. Nadjo, *Inorg. Chem.*, 2010, **49**, 7001.
18. M. Sadakane and E. Steckhan, *Chem. Rev.*, 1998, **98**, 219.
19. P. J. Richardt, R. W. Gable, A. M. Bond and A. G. Wedd, *Inorg. Chem.*, 2001, **40**, 703.
20. S. Himeno, M. Takamoto and T. Ueda, *J. Electoanal. Chem.*, 2000, **485**, 49.
21. M. Takamoto, T. Ueda and S. Himeno, *J. Electoanal. Chem.*, 2002, **521**, 132.
22. S. Himeno, M. Takamoto, T. Ueda, R. Santo and A. Ichimura, *Electoanal.*, 2004, **16**, 656.
23. A. M. Bond, T. Vu and A. G. Wedd, *J. Electoanal. Chem.*, 2000, **494**, 96.
24. B. Keita, D. Bouaziz and L. Nadjo, *J. Electrochem. Soc.*, 1988, **135**, 87.
25. G. Bernardini, A. G. Wedd, C. Zhao and A. M. Bond, *Dalton Trans.*, 2012, **41**, 9944.
26. J. Zhang and A. M. Bond, *Inorg. Chem.*, 2004, **43**, 8263.
27. V. Gutmann, *The Donor-Acceptor Approach to Molecular Interactions*, Plenum Press, New York, 1978.
28. J. Zhang, A. M. Bond, D. R. MacFarlane, S. A. Forsyth, J. M. Pringle, A. W. A. Mariotti, A. F. Glowinski and A. G. Wedd, *Inorg. Chem.*, 2005, **44**, 5123.
29. G. Bernardini, C. Zhao, A. G. Wedd and A. M. Bond, *Inorg. Chem.*, 2011, **50**, 5899.
30. M. Sadakane and E. Steckhan, *Acta Chem. Scand.*, 1999, **53**, 837.

31. B. Keita and L. Nadjo, *J. Electroanal. Chem.*, 1987, **227**, 77.
32. B. Keita and L. Nadjo, *J. Mol. Catal. A*, 2007, **262**, 190.
33. C. Besson, S.-W. Chen, R. Villanneau, G. Izzet and A. Proust, *Inorg. Chem. Commun.*, 2009, **12**, 1042.
34. C. Rigaku, *CrystalStructure 4.0: Crystal Structure Analysis Package*, (2000-2011), Tokyo 196-8666, Japan.
35. G. M. Sheldrick, *Acta Crystallogr. Sect. A*, 2008, **64**, 112.
36. M. Sadakane and M. Higashijima, *Dalton Trans.*, 2003, 659.
37. I. D. Brown and D. Altermatt, *Acta Crystallogr. Sect. B: Struct. Sci.*, 1985, **41**, 244.
38. K. Uehara, K. Fukaya and N. Mizuno, *Angew. Chem. Int. Ed.*, 2012, **51**, 7715.
39. C. C. Rong, H. So and M. T. Pope, *Eur. J. Inorg. Chem.*, 2009, 5211.
40. A. J. Bard and L. R. Faulkner, *Electrochemical Methods*, Wiley, New York, 1980.
41. K. Izutsu, *Electrochemistry in Nonaqueous Solutions*, 2nd edn., Wiley-VCH Verlag GmbH & Co. KGaA, Weinheim, 2009.
42. C. Reichardt, *Solvents and Solvent Effects in Organic Chemistry*, 2nd edn., Wiley-VCH, Weinheim, 1998.
43. C. J. Timpson, C. A. Bignozzi, B. P. Sullivan, E. M. Kober and T. J. Meyer, *J. Phys. Chem.*, 1996, **100**, 2915.
44. D. A. Freedman, D. E. Janzen and K. R. Mann, *Inorg. Chem.*, 2001, **40**, 6009.

Preparation and structural characterisation of tetrabutylammonium salt of mono-ruthenium(III)-substituted α-Keggin-type silicotungstates with 4,4'-bipyridine ligand and its electrochemical behaviour in organic solvents.

Shuhei Ogo,[1] Sachie Moroi,[1] Tadaharu Ueda,[2] Kenji Komaguchi,[1] Shinjiro Hayakawa,[1] Yusuke Ide,[1] Tsuneji Sano[1] and Masahiro Sadakane*[1,3]

1) Department of Applied Chemistry, Graduate School of Engineering, Hiroshima University, 1-4-1 Kagamiyama, Higashi-Hiroshima, 739-8527, Japan

2) Department of Chemistry, Faculty of Science, Kochi University, 2-5-1 Akebono-cho, Kochi 780-8520, Japan

3) Japan Science and Technology Agency (JST), PRESTO, 4-1-8 Honcho, Kawaguchi, Saitama, 332-0012, Japan

Instrumentation

Room-temperature Ru L_3-edge XANES spectra were measured at the BL11 beamline of the Hiroshima Synchrotron Research Center (HSRC).[1] The storage ring was operated at 700 MeV, and the synchrotron radiation from a bending magnet was monochromatized with a Si-(111) double-crystal monochromator. The sample chamber was filled with He, and a sample was mounted on a copper holder connected to a current amplifier. The angle between the incident X-rays and the sample surface was 20º. The X-ray fluorescence yield (XFY) from the sample was measured with a commercial Silicon drift detector (Amptek, XR-100SDD). XANES spectra were recorded from 2825 to 2855 eV with an energy step of 0.25 eV. The sample holder was a copper plate 0.2 mm thick, and it had a hole in the center that was 15 mm in diameter. Powder of the sample was supported on a piece of adhesive tape attached to the hole in the holder.

Electron spin resonance (ESR) spectra were recorded at 77 K on a JEOL JES-RE1X and Bruker ESP300E spectrometers (X-band). Spectra simulation was done by Bruker SimFonia software package. The sample was dissolved in solvent (ca. 0.5 mM) and a proper amount of the solution was placed into a Suprasil quartz tube (ϕ = 5 mm). The quartz tube was sealed after several degassed-and-thaw cycles on a vacuum

line.

Cyclic voltammetry (CV) and differential pulse voltammetry (DPV) in aqueous solution were performed on a BAS 50W system at ambient temperature. A glassy carbon working electrode (diameter, 3 mm), a platinum wire counter electrode and an Ag/AgCl reference electrode (203 mV vs NHE at 25 ºC) (3M NaCl, Bioanalytical Systems, Inc.) were used. The voltage scan rate was set at 25 mV s^{-1}. Approximate formal potential values $E_{1/2}$ were calculated from the cyclic voltammograms as the average of cathodic and anodic peak potentials for corresponding oxidation and reduction waves.

Table S1 Experimental ESR parameters of **1**

Solvents[a]	g_1	g_2	g_3	g_{iso}
Acetone	2.590	2.366	1.560	2.172
DMF	2.587	2.368	1.560	2.172
DMSO	2.605	2.370	1.520	2.165
Acetonitrile	2.585	2.370	1.560	2.172

[a] DMF: *N*,*N*-dimethylformamide and DMSO: dimethylsulfoxide.

Table S2 Experimental ESR parameters in acetonitrile solution at 77 K

Sample[a]	g_1	g_2	g_3	g_{iso}	Ref.
$[SiW_{11}O_{39}Ru^{III}(bipy)]^{5-}$ (**1**)	2.585	2.370	1.560	2.172	This work
$[PW_{11}O_{39}Ru^{III}(py)]^{4-}$	2.579	2.338	1.603	2.173	[2]
$[PW_{11}O_{39}Ru^{III}(DMSO)]^{4-}$	2.296	2.192	1.877	2.122	[2]

[a] bipy: 4,4'-bipyridine, py: pyridine and DMSO: dimethylsulfoxide.

Stability of 1 in organic solvents

TBA salt of **1** was purified from acetonitrile solution. Single crystal structural analysis indicated that bipyridine was coordinated to Ru in $SiW_{11}O_{39}Ru$ (Fig. 1). IR spectrum shows that the **1** contained bipyridine ligand and TBA cations (Fig. S1). It was confirmed that the valence of the ruthenium ion in **1** was +3 by using the Ru-L_3-edge XANES technique (Fig. S2). ^{1}H-NMR spectrum suggested that the presences of bipyridine ligand coordinating to paramagnetic Ru^{III} and TBA cations with molar ratio of 1:5 (Fig. S4). Moreover, ESR spectrum and the g_{iso} value (2.172) of **1** in acetonitrile

solution were almost the same as those of $TBA_4[PW_{11}O_{39}Ru^{III}(py)]$ (g_{iso} = 2.173) (Fig. S5 and Table S2).[2] These results indicated that the compound **1** was stable in acetonitrile. In addition, ESR spectra and g_{iso} values in acetone, DMF and DMSO were almost the same as those in acetonitrile (Fig. S5 and Table S1). It was reported that g_{iso} values for $[PW_{11}O_{39}Ru^{III}(py)]^{4-}$ and $[PW_{11}O_{39}Ru^{III}(DMSO)]^{4-}$ were different (Table S2).[2] This result indicated that the compound **1** was also stable in these organic solvents. The UV-Vis spectra were almost same after storing six months, indicating **1** was stable in these solvents (Fig. S9).

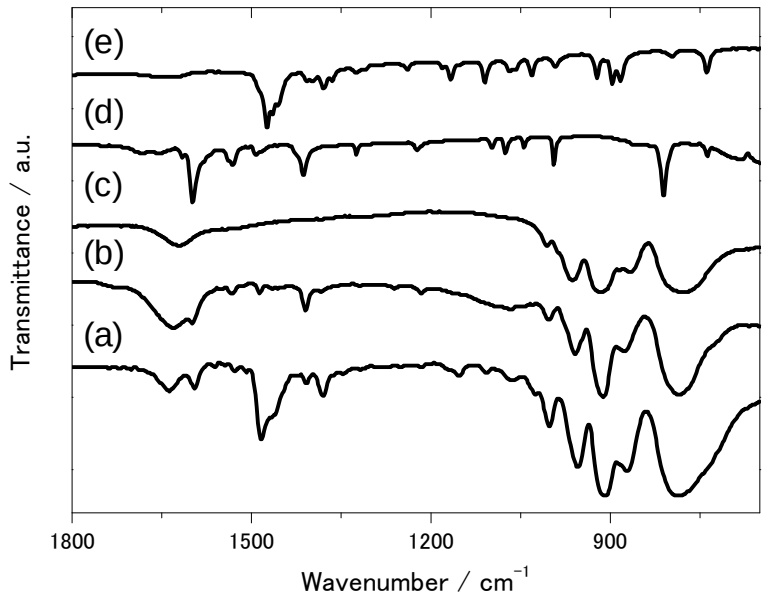

Fig. S1. FT-IR spectra of (a) **1**, (b) $Cs_5[\alpha\text{-}SiW_{11}O_{39}Ru^{III}(bipy)]$, (c) $Cs_5[\alpha\text{-}SiW_{11}O_{39}Ru^{III}(H_2O)]$, (d) 4,4'-bipyridine and (e) tetrabutylammonium bromide.

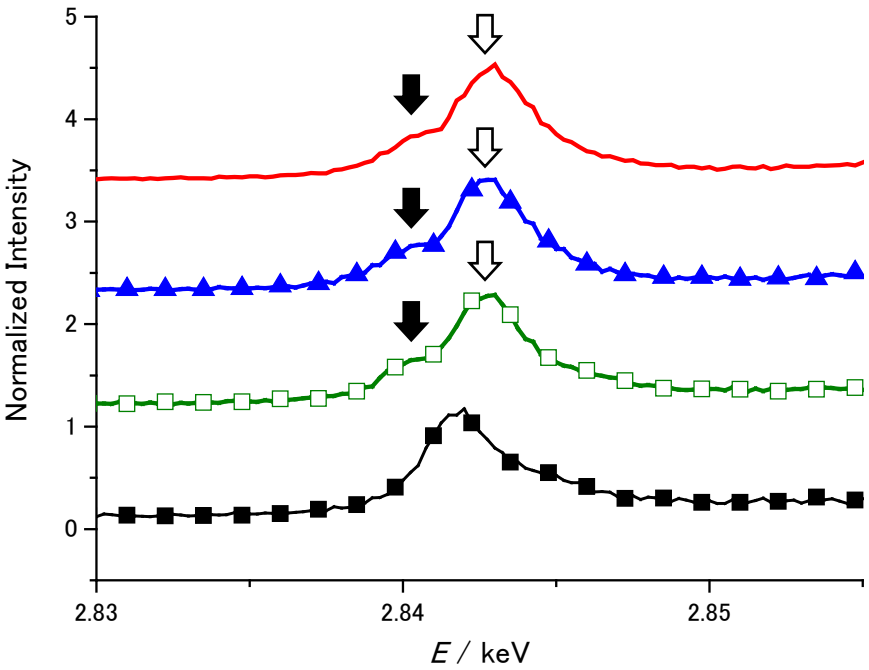

Fig. S2. Normalised XANES spectra at the Ru-L_3-edge. (red line) **1**, (blue line with closed triangles) $Cs_5[SiW_{11}O_{39}Ru^{III}(pyridine)]$, (green line with open squares) $Cs_4[PW_{11}O_{39}Ru^{III}(dmso)]$ and (black line with closed squares) $Cs_5[PW_{11}O_{39}Ru^{II}(dmso)]$. The white and black arrows indicate the peak correspond to e_g and t_{2g}, respectively.

Ru L_3-edge XANES spectra

We confirmed the valence of ruthenium in **1** using the X-ray absorption near edge spectra (XANES) technique. It is widely known that chemical shift of the absorption edge shows a simple relation as a function of the oxidation state of the element of interest. We previously reported Ru K-edge and L-edge XANES of $Cs_5[SiW_{11}O_{39}Ru^{III}(pyridine)]$,[3] $Cs_4[PW_{11}O_{39}Ru^{III}(dmso)]$ (dmso = dimethyl sulfoxide) and $Cs_5[PW_{11}O_{39}Ru^{II}(dmso)]$.[4]

The L_3-edge absorption corresponds to transitions from $2p_{3/2}$ (L_3) to an unoccupied d states, and a Ru L_3-edge spectrum reflects the local coordination of Ru and the number of 4d electrons. All investigated Ru compounds have octahedral coordination with low-spin, and two peaks in the spectra correspond to e_g (white arrows) and t_{2g} (black arrows). The peak separation is related to the crystal field strength, and the relative intensity of the t_{2g} peak indicates the number of 4d electrons.[5-7] The peak shape of **1** is similar to the peak shapes of $Cs_5[SiW_{11}O_{39}Ru^{III}(pyridine)]$ and $Cs_4[PW_{11}O_{39}Ru^{III}(dmso)]$ in full agreement with a +3 valence of ruthenium in **1**.

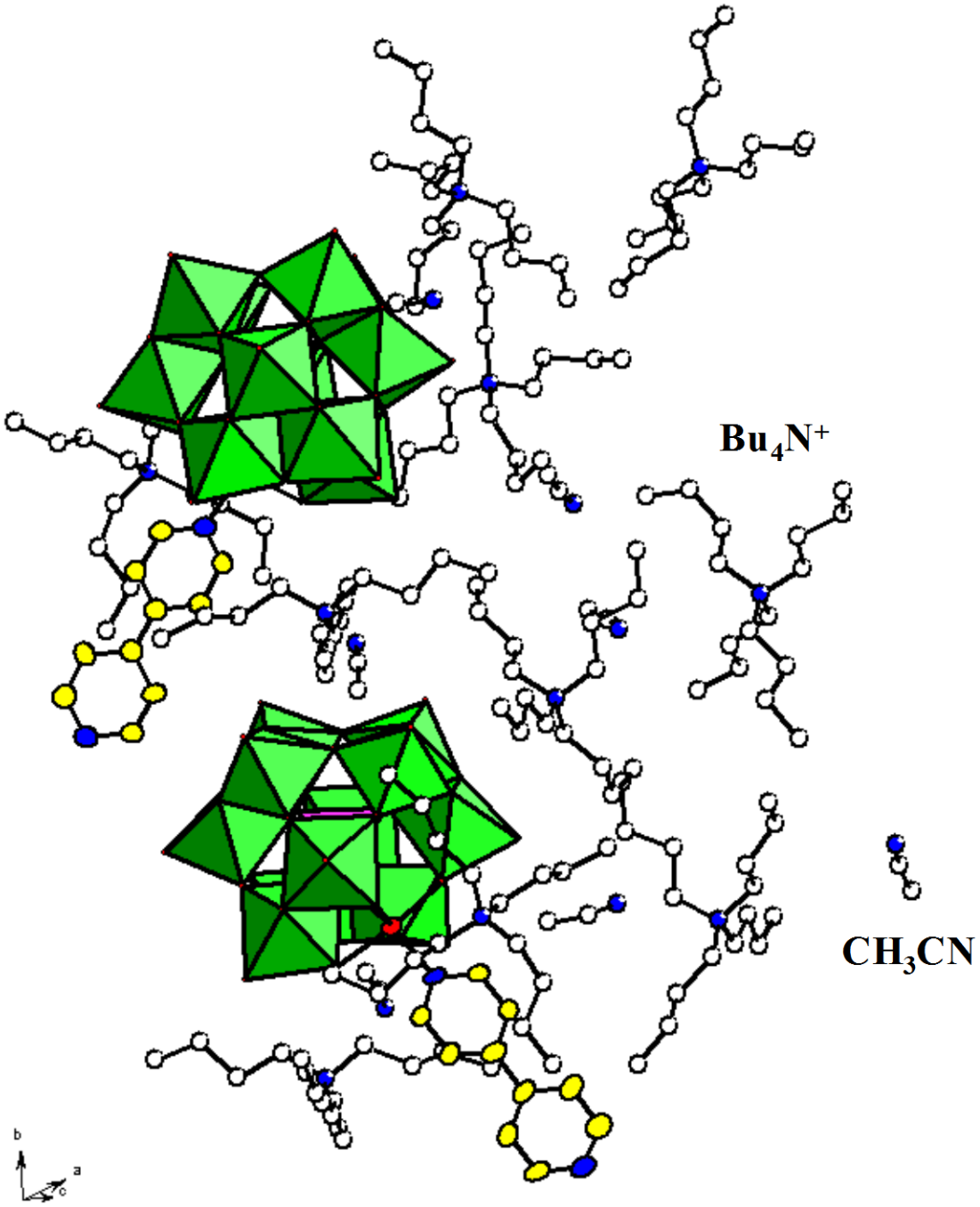

Fig. S3. Crystal packing of **1**. Colour code: C white (C of bipyridine-ring yellow), N blue and Ru red balls, SiO_4 blue tetrahedral and WO_6 green octahedral.

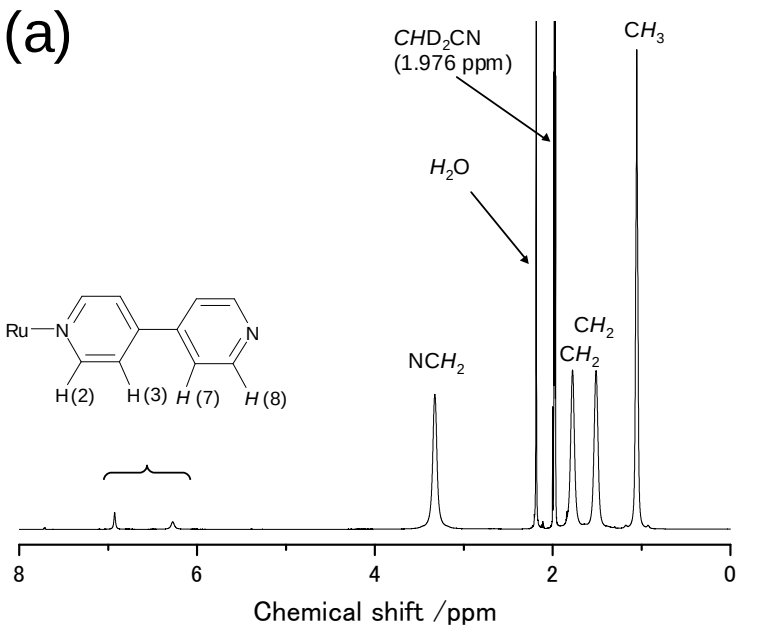

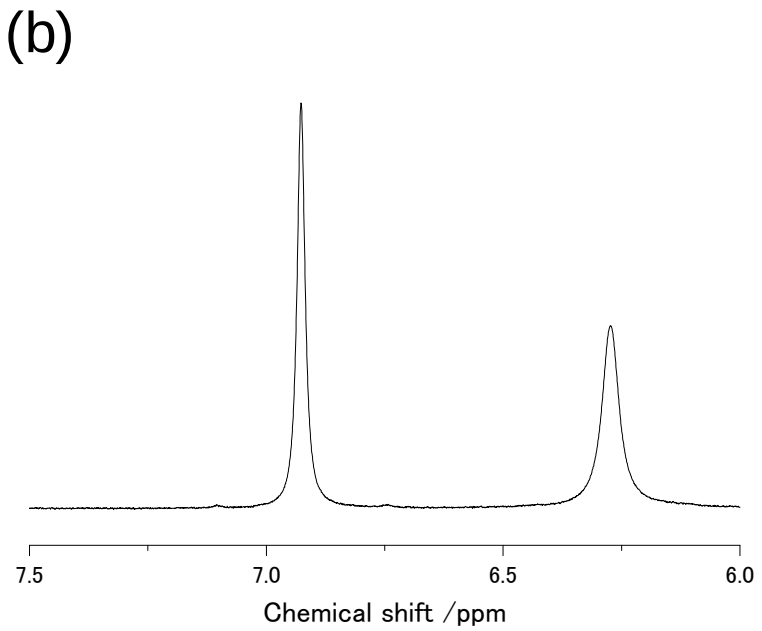

Fig. S4. (a) ^{1}H-NMR spectrum of **1** and (b) its expanded spectrum.

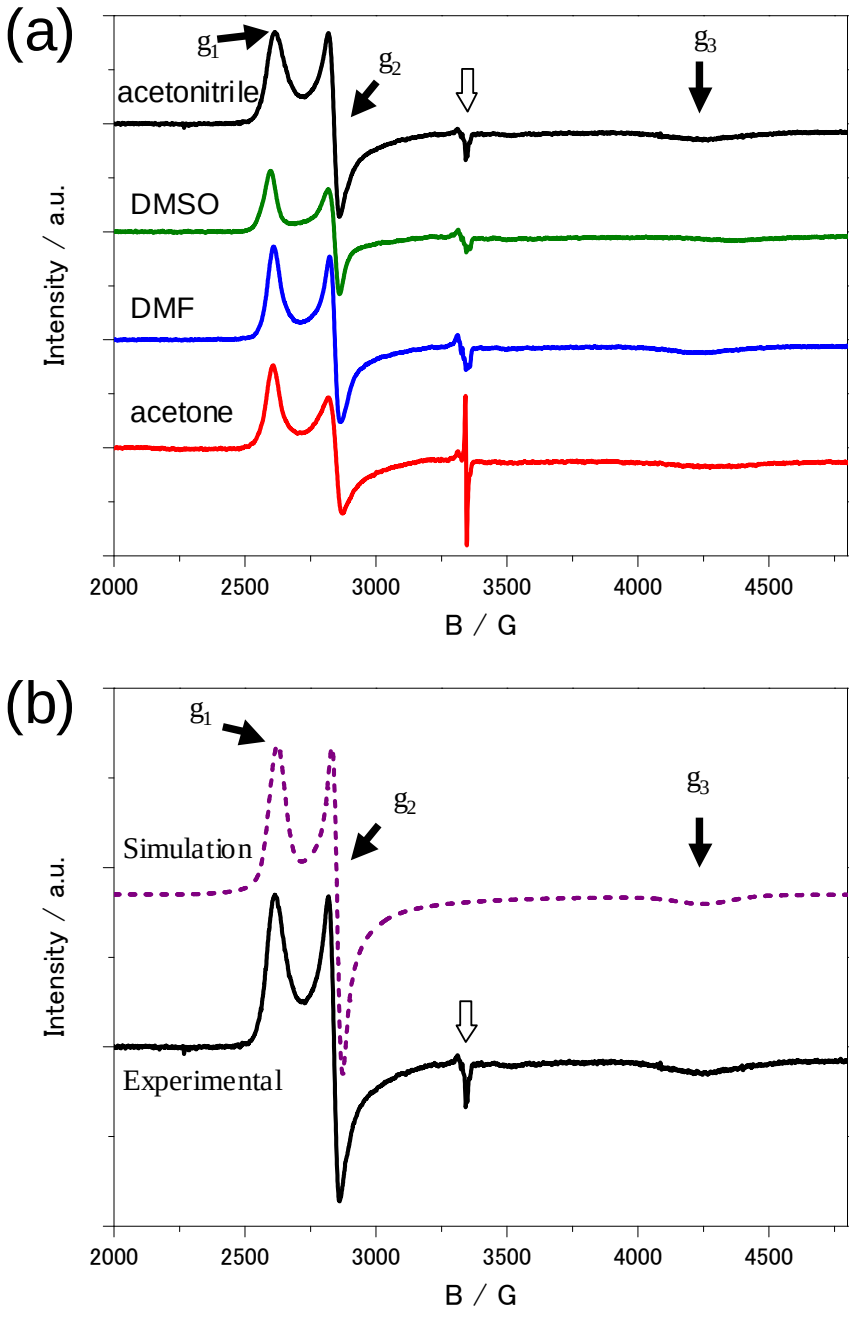

Fig. S5. (a) ESR spectra of **1** in the organic solvents at 77 K. (b) Experimental and simulated ESR spectra of **1** in acetonitrile at 77 K. DMF is *N*,*N*-dimethylformamide and DMSO is dimethylsulfoxide. White arrow indicates unknown peak.

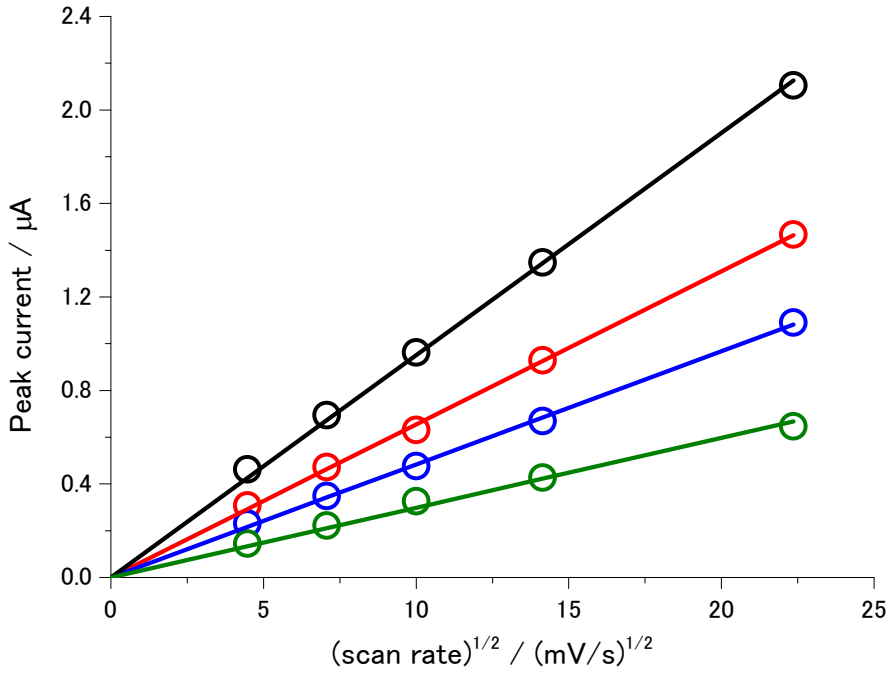

Fig. S6. Oxidation peak currents of $Ru^{IV/III}$-bipy in various organic solvents plotted against $(\text{scan rate})^{1/2}$. (red) acetone, (blue) *N*,*N*-dimethylformamide (DMF), (green) dimethylsulfoxide (DMSO) and (black) acetonitrile.

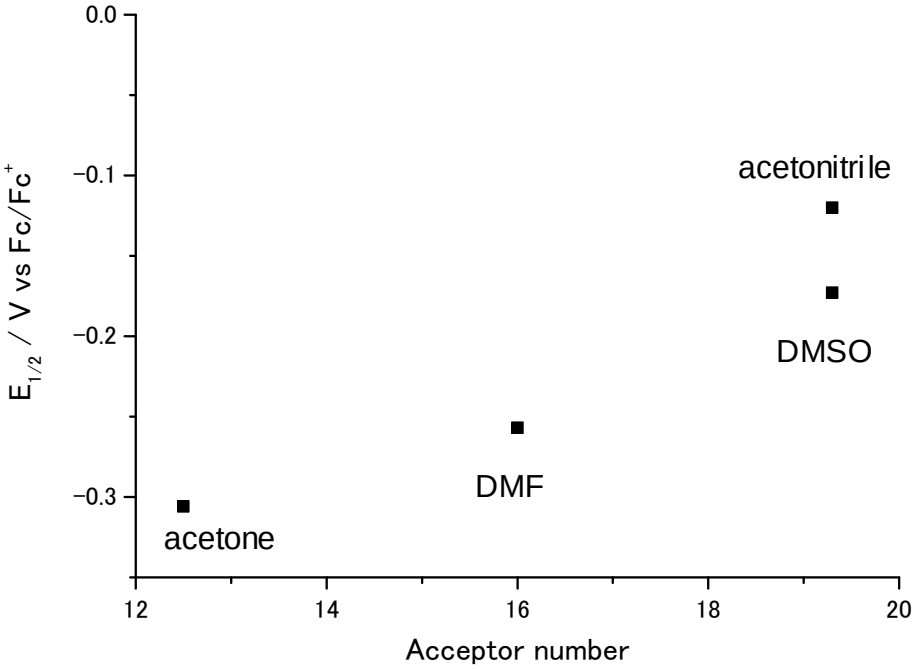

Fig. S7. Relationship between the redox potential of $Ru^{IV/III}$ and the acceptor number of solvents studied. DMF is *N*,*N*-dimethylformamide and DMSO is dimethylsulfoxide.

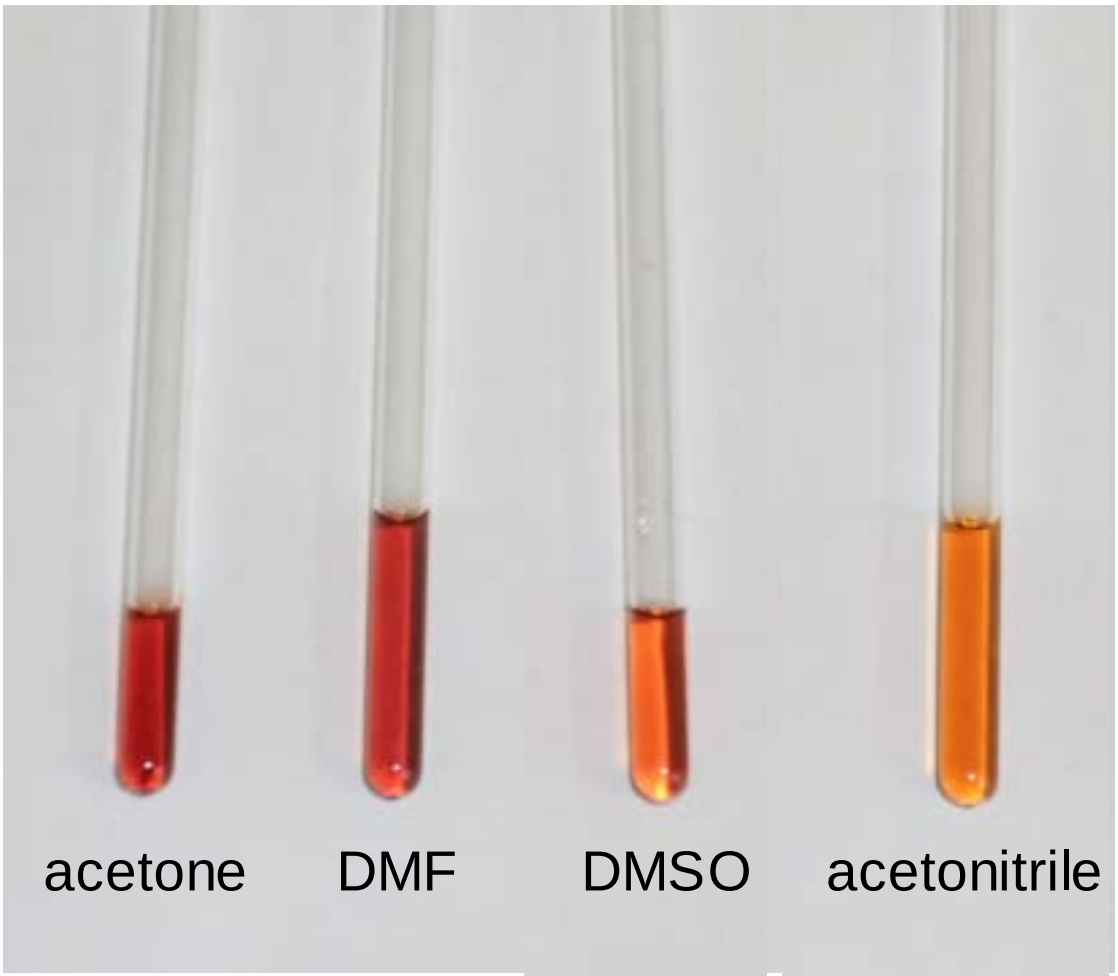

Fig. S8. Photograph of **1** dissolved in various organic solvents. DMF is *N*,*N*-dimethylformamide and DMSO is dimethylsulfoxide.

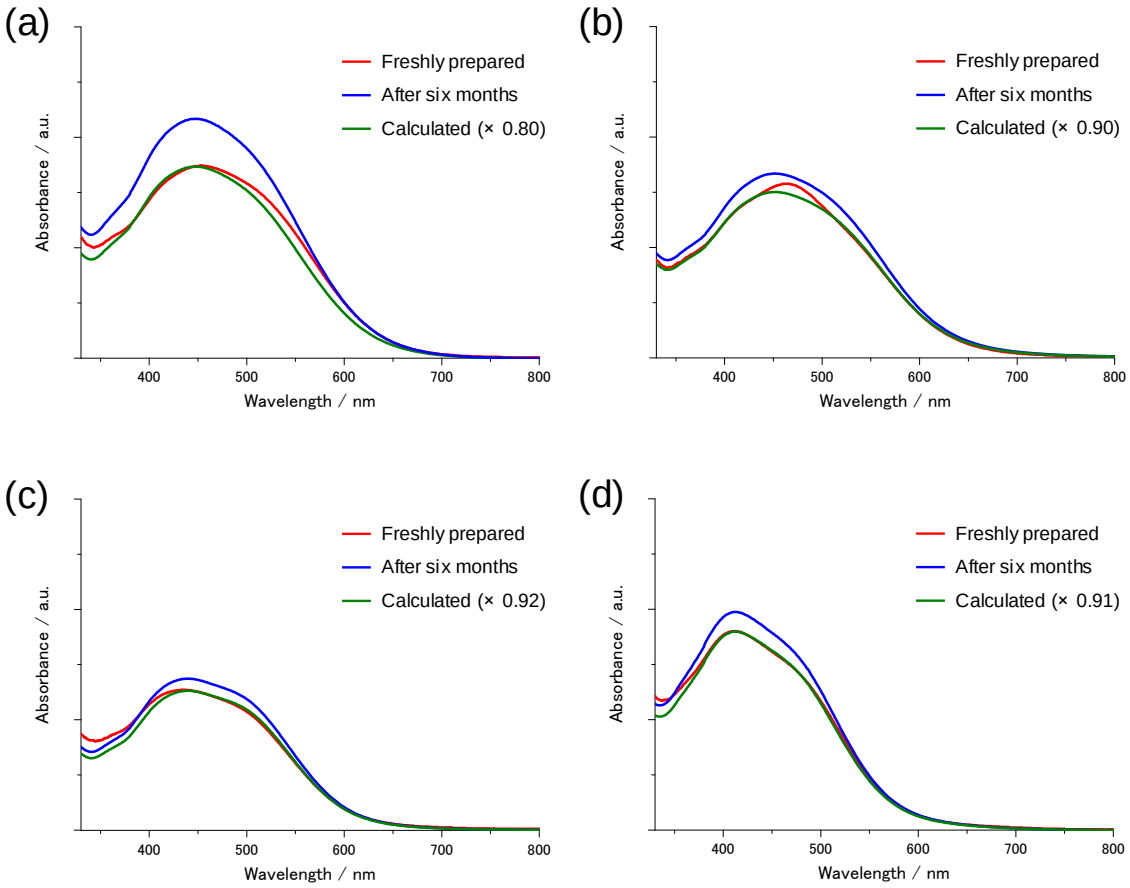

Fig. S9. UV-Vis spectra of **1** in (a) acetone, (b) DMF, (c) DMSO and (d) acetonitrile. UV-Vis spectra of (red) freshly prepared solution and (blue) the solution after storing six months, and (green) calculated UV-Vis spectra. DMF is *N*,*N*-dimethylformamide and DMSO is dimethylsulfoxide.

UV-Vis spectra of 1 in the organic solvents after storing six months

In order to prove stability of **1** in the organic solvents, UV-Vis spectra of **1** dissolved in the organic solvents and UV-Vis spectra of **1** in the solution which was stored six months were compared. In all solvents, UV-Vis absorbance of the stored solution was higher than the freshly prepared solution due to evaporation of solvents. The calculated

spectra, which were estimated by considering evaporation, gave close agreement with the spectra of freshly prepared solution within the range of 400-800 nm, except for the DMF solution, in which the absorption band at around 480 nm was slightly decreased. Although **1** might be slightly decomposed in DMF, **1** was stable in the organic solvents.

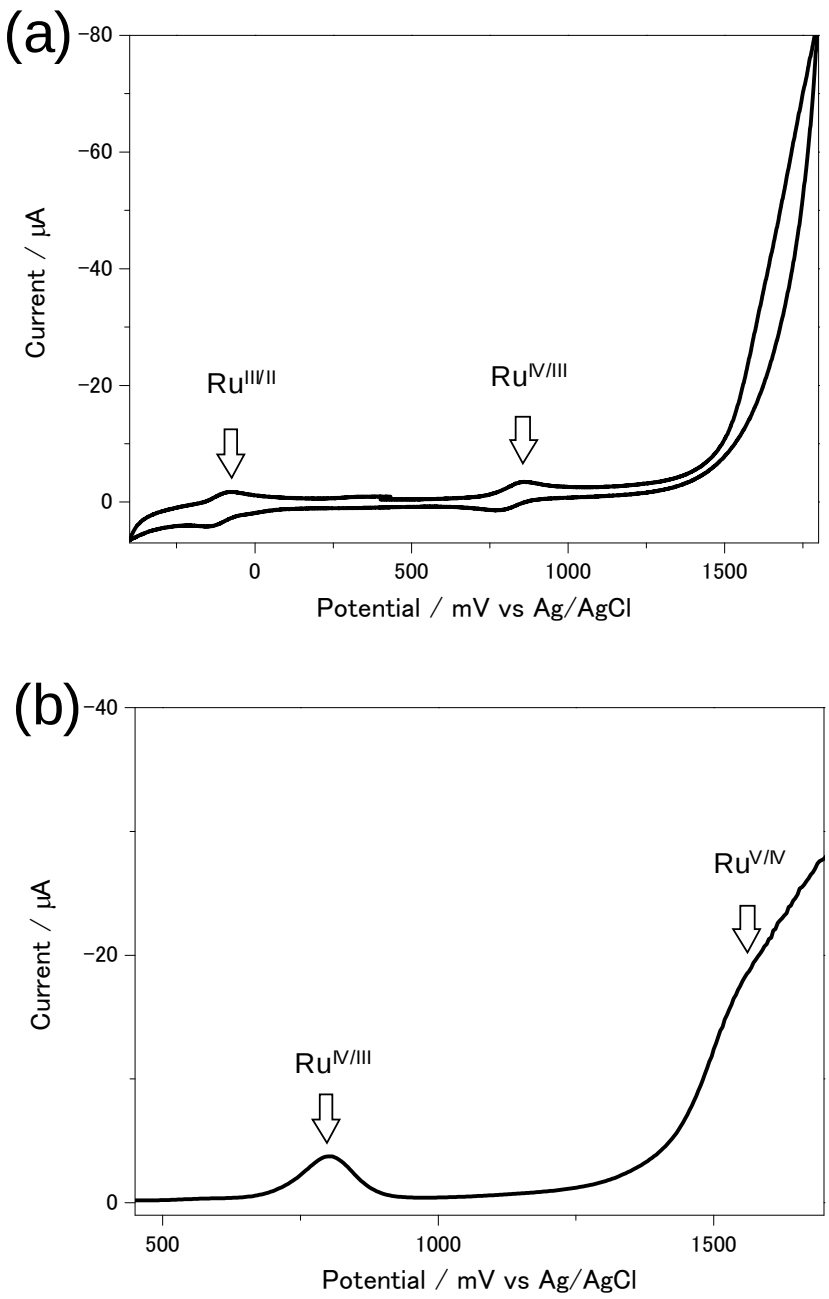

Fig. S10. (a) CV and (b) DPV curves of $Cs_5[SiW_{11}O_{39}Ru(bipy)]$ in 0.5 M KH_2PO_4 aqueous solution (pH 6.54).

References

1. S. Hayakawa, Y. Hajima, S. Qian, H. Namatame and T. Hirokawa, *Anal. Sci.*, 2008, **24**, 835.
2. C. C. Rong, H. So and M. T. Pope, *Eur. J. Inorg. Chem.*, 2009, 5211.
3. M. Sadakane, S. Moroi, Y. Iimuro, N. Izarova, U. Kortz, S. Hayakawa, K. Kato, S. Ogo, Y. Ide, W. Ueda and T. Sano, *Chem. Asia. J.*, 2012, **7**, 1331.
4. M. Sadakane, N. Rinn, S. Moroi, H. Kitatomi, T. Ozeki, M. Kurasawa, M. Itakura, S. Hayakawa, K. Kato, M. Miyamoto, S. Ogo, Y. Ide and T. Sano, *Z. Anorg. Allgem. Chem.*, 2011, **637**, 1467.
5. F. M. F. de Groot, *Physica B*, 1995, **208&209**, 15.
6. Z. Hu, H. von Lips, M. S. Golden, J. Fink, G. Kaindl, F. M. F. de Groot, S. Ebbinghaus and A. Reller, *Phys. Rev. B*, 2000, **61**, 5262.
7. T. K. Sham, *J. Am. Chem. Soc.*, 1983, **105**, 2269.